International Journal of
Molecular Sciences

MDPI

Article

Facile Histamine Detection by Surface-Enhanced Raman Scattering Using SiO_2@Au@Ag Alloy Nanoparticles

Kim-Hung Huynh [1], Xuan-Hung Pham [1], Eunil Hahm [1], Jaehyun An [1], Hyung-Mo Kim [1], Ahla Jo [1], Bomi Seong [1], Yoon-Hee Kim [1], Byung Sung Son [1], Jaehi Kim [1], Won-Yeop Rho [2] and Bong-Hyun Jun [1,*]

[1] Department of Bioscience and Biotechnology, Konkuk University, Seoul 143-701, Korea; huynhkimhung82@gmail.com (K.-H.H.); phamricky@gmail.com (X.-H.P.); greenice@konkuk.ac.kr (E.H.); wogus4067@naver.com (J.A.); hmkim0109@konkuk.ac.kr (H.-M.K.); iamara0421@konkuk.ac.kr (A.J.); bom826@naver.com (B.S.); yoonhees@konkuk.ac.kr (Y.-H.K.); imsonbs@konkuk.ac.kr (B.S.S.); susia45@gmail.com (J.K.)

[2] School of International Engineering and Science, Jeonbuk National University, 567 Baekje-daero, Deokjin-gu, Jeonju-si, Jeollabuk-do 54896, Korea; rho7272@jbnu.ac.kr

* Correspondence: bjun@konkuk.ac.kr; Tel.: +82-2-450-0521

Received: 31 March 2020; Accepted: 3 June 2020; Published: 5 June 2020

Abstract: Histamine intoxication associated with seafood consumption represents a global health problem. The consumption of high concentrations of histamine can cause illnesses ranging from light symptoms, such as a prickling sensation, to death. In this study, gold–silver alloy-embedded silica (SiO_2@Au@Ag) nanoparticles were created to detect histamine using surface-enhanced Raman scattering (SERS). The optimal histamine SERS signal was measured following incubation with 125 μg/mL of SiO_2@Au@Ag for 2 h, with a material-to-histamine solution volume ratio of 1:5 and a phosphate-buffered saline-Tween 20 (PBS-T) solvent at pH 7. The SERS intensity of the histamine increased proportionally with the increase in histamine concentration in the range 0.1–0.8 mM, with a limit of detection of 3.698 ppm. Our findings demonstrate the applicability of SERS using nanomaterials for histamine detection. In addition, this study demonstrates that nanoalloys could have a broad application in the future.

Keywords: histamine; fish; gold-silver alloy-embedded silica nanoparticles; surface-enhanced Raman scattering (SERS); reliable and sensitive detection

1. Introduction

Histamine is a common biological substance involved in immune responses, physiological function, and neurotransmission. The consumption of high concentrations of histamine can cause illness ranging from light symptoms, such as a prickling or burning sensation, to serious symptoms, such as erythema, vomiting, diarrhea, headache, angioedema, and urticaria, and even shock or death. Nearly all cases of histamine poisoning are associated with the consumption of fish containing high levels of histidine, which is easily transformed to histamine by decarboxylation if the fish is not correctly stored. Once histamine is produced, it is not easy to completely remove it by heat treatment or freezing. In addition, histamine has no color or odor, which hinders the identification of histamine contamination without noticeable changes in the appearance or smell of the fish [1–5]. According to the European Union (EU) and

the U.S. Food and Drug Administration (FDA) standards, the concentration of histamine in fish for consumption must be <100 and 50 ppm, respectively. Therefore, reliable, rapid detection of histamine in fish is essential for food safety and public health, as well as for the global fish industry. Generally, histamine detection is performed using methods such as high-performance liquid chromatography (HPLC), capillary electrophoresis (CE), enzyme linked immunosorbent assay (ELISA), fluorescence quantification, and ion exchange chromatography [6–11]. Although these methods are very sensitive, they do have some disadvantages; they use hazardous chemicals and require lengthy pretreatment or specific enzymes, which are expensive and strictly produced. In addition, some protocols indirectly detect histamine via histamine derivatives, which can lead to incorrect results [3,6,7].

Surface-enhanced Raman scattering (SERS) is a spectroscopic technique discovered in the 1970s. SERS is an ideal analysis technique, as it can detect single molecules, as well enhance the chemical molecule signal by up to 10^{16}-fold. Compared with other analysis methods, SERS requires simple sample preparation and can use a wide range of excitation frequencies, which enables less energetic excitation, resulting in reduced photodamage. Metal colloids, typically silver or gold colloids in suspension or aggregation, have been broadly used for SERS measurements owing to their strong SERS signal and low toxicity [12–14]. The useful application of SERS has motivated researchers to develop more reliable SERS techniques. Among those techniques under development, nanoalloy materials have been successfully produced. The abundant variety of metallic alloy compositions, structures, and properties, which can consist of bimetallic nanoclusters (Cu-Ag, Cu-Au, Ag-Au, Ni-Pt, and Fe-Ni) or trimetallic nanoclusters (Cu-Au-Pt, Pd-Ag-Fe, Au-Pt-Ag, and Pd-Au-Pt), has created better stability and synergism that has enabled their widespread application in electronics, engineering, and catalysis [15–19].

Currently, SERS is being increasingly applied in the field of food safety for the detection of harmful substances. Several studies have used silver or gold colloids to detect histamine by SERS [1–5]. Compared with other standard methods, such as HPLC, these SERS methods have the advantages of sensitivity, reliability, and easy fabrication; however, precise control of the size and amount of the aggregated particle clusters is difficult because of the heterogeneous formation of the metal particles. The use of a template, such as silica particles or polymer beads, to accumulate silver or gold nanoparticles (NPs) has been widely established in order to control particle size [20–28]. Recently, our group produced an Au-Ag alloy on silica nanoparticles as a highly sensitive and reliable SERS probe that can detect molecular targets at very low concentrations [29–42]. Based on these studies, we investigated histamine detection using an Au-Ag alloy on silica particles as a material for SERS.

2. Results and Discussion

2.1. Characterization of the SiO_2@Au@Ag NPs

The SiO_2@Au@Ag NP material was prepared based on studies conducted by the Pham group revealing that SiO_2@Au@Ag NPs exhibit a high Raman enhancement effect [39,43,44]. Silica NPs were produced using the Stöber method. Subsequently, the surfaces of the silica NPs were covered with Au NPs on which an Ag shell was created.

Figure 1 shows transmission electron microscopy (TEM) images of the nanomaterials. The average diameter of the SiO_2 NPs was 160 nm (1a). SiO_2 NPs covered by Au NPs (2–3 nm) are shown in Figure 1b. The surface of the SiO_2@Au NPs was thoroughly coated with an Ag shell (1c), with clear nanogaps between the Ag NPs, which will provide the best Raman signal [39]. As shown in Figure 1d, while the SiO_2 suspension did not exhibit UV–Vis absorbance in the 300–1000 nm range, the SiO_2@Au NP colloid showed a peak at approximately 520 nm. Once the Ag NPs were embedded onto SiO_2@Au, the absorbance of the SiO_2@Au@Ag suspension showed a wide band from 320 to nearly 800 nm.

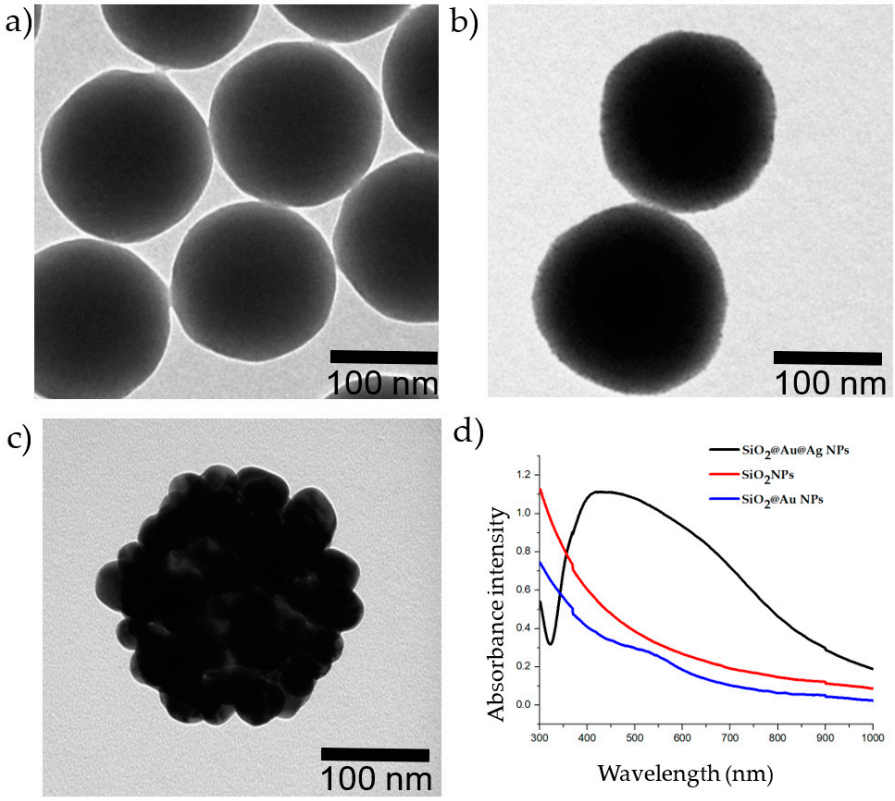

Figure 1. Images of the nanoparticles and UV–Vis absorbance of the nanoparticles. (**a**) Transmission electron microscopy (TEM) image of silica (SiO_2) NPs; (**b**) TEM image of SiO_2@Au NPs; (**c**) TEM image of SiO_2@Au@Ag NPs; (**d**) UV–Vis absorbance of NPs. Red: 1000 μg/mL SiO_2 NPs; blue: 250 μg/mL SiO_2@Au NPs; black: 20 μg/mL SiO_2@Au@Ag NPs.

2.2. Optimization of Histamine Detection

As the SERS signal is affected by many factors, we sought to determine the effect of target volume, incubation time, solvent pH, and material concentration on SERS signal. The SERS spectra of histamine-modified SiO_2@Au@Ag were observed at 850, 1001, 1200, 1258, 1263, 1318, 1353, 1449, 1536, 1603, and 1641 cm^{-1} (Figure S1 and Table S1, Supplementary Materials). The bands at 1641, 1603, 1536, 1353, and 850 cm^{-1} were assigned to ring stretching; the bands at 1258 and 1001 cm^{-1} were assigned to ring bending; the band at 1449 cm^{-1} was assigned to the bending of the CH_2 side chain; the band at 1318 cm^{-1} was assigned to CH_2 wagging; and the bands at 1200 and 1263 cm^{-1} were assigned to ring breathing [45–50]. For simple evaluation, we considered an intensity of wavelength number of 1603 cm^{-1}, which might be due to ring stretching [45–50], as the highest histamine Raman shift peak.

2.2.1. Effect of Target Volume on Histamine Detection

As the SERS signal is affected by the amount of target molecule on the surface of the material, we carried out an experiment in which we incubated 20 μg of SiO_2@Au@Ag NPs (100 μL) with different volumes of 1 mM histamine (100, 500 μL, and 1000 μL); the mean ratio between the volume of the material and histamine was 1:1, 1:5, and 1:10, respectively. As shown in Figure 2, the SERS signal increased with increasing volume, as the amount of histamine absorbed onto the surface of the material increased. Therefore, the SERS signal at a 1:5 and 1:10 ratio was clearer than that at a 1:1 ratio. The 1:5 ratio was chosen for subsequent experiments.

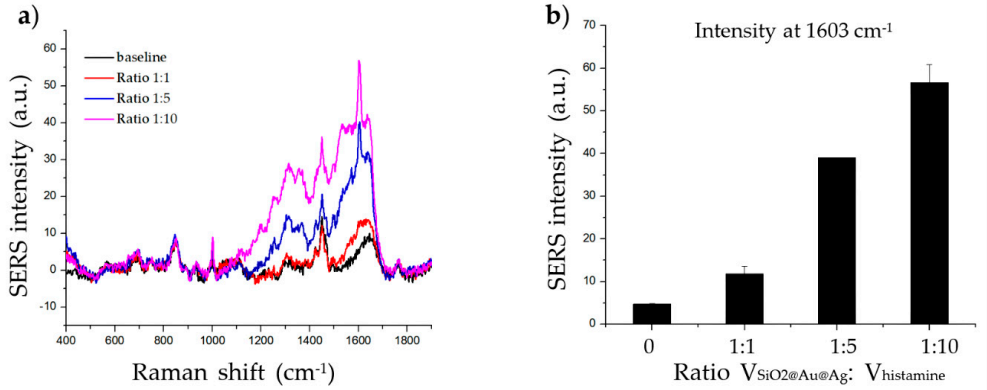

Figure 2. Effect of target volume on histamine detection. (**a**) Raman signal of histamine incubated with SiO_2@Au@Ag nanoparticles (NPs) at three volume ratios (1:1, 1:5, and 1:10) after 2 h. (**b**) The Raman intensity of histamine incubated with SiO_2@Au@Ag NPs at various volume ratios after 2 h (at 1603 cm^{-1}).

2.2.2. Effect of Incubation Time on Histamine Detection

The incubation step allows the target molecule to adsorb onto the surface of the material. To determine the effect of histamine incubation time, histamine was incubated with 20 µg of material for 0, 0.5, 1, 2, 4, 6, and 8 h. As shown in Figure 3, the intensity of the SERS signal increased up to 1 h of incubation. After 1 h, the SERS signal of the histamine gradually increased with further incubation. The signals at wave number 1603 cm^{-1} are clear enough irrespective of experimental incubation time; thus, 2 h of incubation was chosen for subsequent experiments as the intensity at 2 h represents approximately the average of the intensity obtained after incubation for the other time periods.

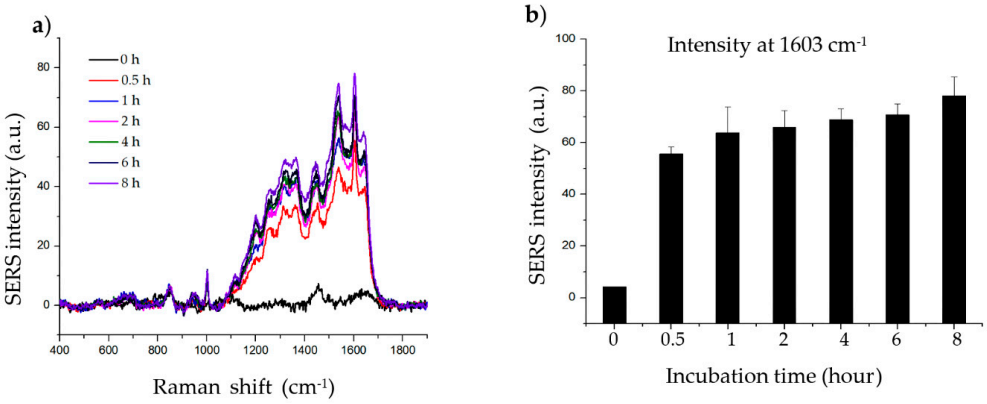

Figure 3. Effect of incubation time on histamine detection. (**a**) Raman signal of histamine incubated with SiO_2@Au@Ag nanoparticles (NPs) after 0.5, 1, 2, 4, 6, and 8 h. (**b**) Raman intensity of histamine incubated with SiO_2@Au@Ag NPs after 0.5, 1, 2, 4, 6, and 8 h (at 1603 cm^{-1}).

2.2.3. Effect of Solvent pH on Histamine Detection

To determine the effect of pH on the SERS signal of the histamine, phosphate-buffered saline-Tween 20 (PBS-T) solvents with various pH values (3, 5, 7, and 9) were created by adjusting the pH with hydrochloric acid (HCl) and sodium hydroxide (NaOH). As shown in Figure 4, the SERS signal of the histamine was strong and clear at all four pH values. However, based on this result, the binding between the histamine and the Ag shell appears to be better in an alkaline environment. Thus, pH 7 was chosen for subsequent experiments as it is near the physiological pH.

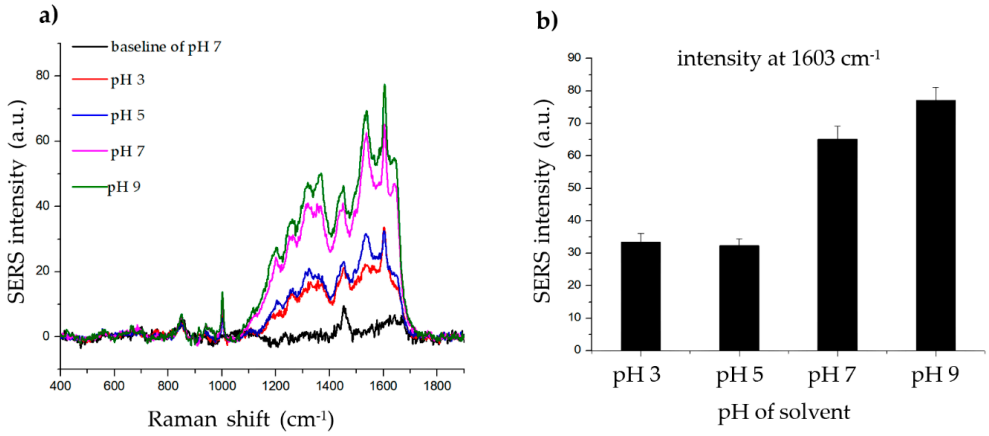

Figure 4. Effect of solvent pH on histamine detection. (**a**) Raman signal of histamine incubated with SiO_2@Au@Ag nanoparticles (NPs) after 2 h in solvents (phosphate-buffered saline-Tween 20 (PBS-T)) with different pH values (3, 5, 7, and 9). (**b**) The Raman intensity of histamine in solvents (PBS-T) with different pH values (3, 5, 7, and 9) (at 1603 cm^{-1}).

2.2.4. Effect of the Material Concentration on the SERS Signal of Histamine

To determine the effect of the material concentration on the SERS signal of histamine, we incubated the same amount of histamine with different concentrations of material (1, 0.5, 0.25, 0.125, and 0.0625 mg/mL) and measured the Raman signal. As shown in Figure 5, the strongest SERS signal was detected when 0.125 mg/mL material was incubated with histamine, while weaker SERS signals were detected at both higher and lower concentrations. These results indicate that the dispersion density of histamine on the surface of the material significantly affected the SERS signal. Although the high and low concentrations of the material did not generate a sufficiently robust SERS signal, any of the concentrations can be used, as the intensities at 1603 cm^{-1} were strong and could be clearly observed.

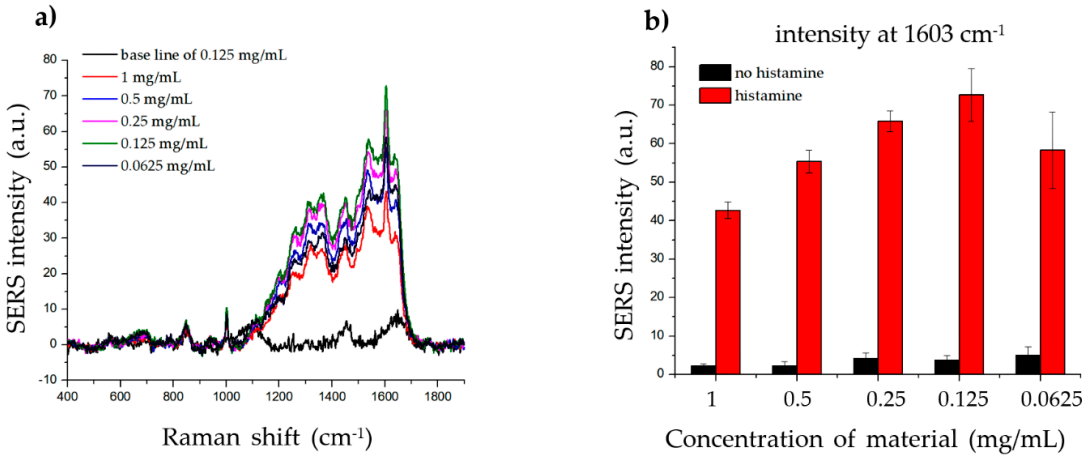

Figure 5. Effect of material concentration on histamine detection. (**a**) The Raman signal of the same concentration of histamine incubated with 1, 0.5, 0.25, 0.125, and 0.0625 mg/mL of SiO_2@Au@Ag nanoparticles (NPs). (**b**) The Raman intensity of histamine for different concentrations of SiO_2@Au@Ag NPs (at 1603 cm^{-1}).

2.3. The Limit of Detection (LOD) of Histamine

To determine the LOD of histamine, we measured the SERS signal at various concentrations of histamine (0.1–0.8 mM) with 20 μg of material (Figure 6a). The intensity at 1603 cm^{-1} increased proportionally with increasing histamine concentration (Figure 6b). The linear calibration formula was determined as y = 37.79951x + 2.89144, R^2 = 0.99081 (x = histamine concentration, y = SERS intensity at 1603 cm^{-1}). The LOD of histamine was 0.033 mM (3.698 ppm) with a signal-to-noise ratio (S/N) = 3, which is considerably lower than the standards described by the FDA (50 ppm) or EU (100 ppm). The LOD of the present method (3.698 ppm) was also comparable to that of existing histamine detection methods such as ELISA (1–17 ppm) [6,8,11], HPLC (0.1–25 ppm) [7,8,10,51], and SERS (5–15 ppm) [2,4,5]. Although the LOD of the present method was not lower than the lowest ELISA and HPLC LODs, it remains useful, as its LOD is lower than the highest LOD values of the other methods. Furthermore, SERS-based methods, including the present method, are suitable for biological applications owing to several advantages, such as low cost, high efficacy, fewer harmful chemicals, non-destructive features, and simple sample preparation. The present method also showed a lower LOD than previous SERS-based histamine detection methods (3.986 vs. 5–15 ppm), owing to the use of Au-Ag alloy NPs instead of Au or Ag NPs. Thus, these results indicate the possible application of this method for histamine detection in fish samples. Additionally, these results also demonstrate a novel SERS-based method using gold-silver alloy-embedded silica NPs for molecular determination.

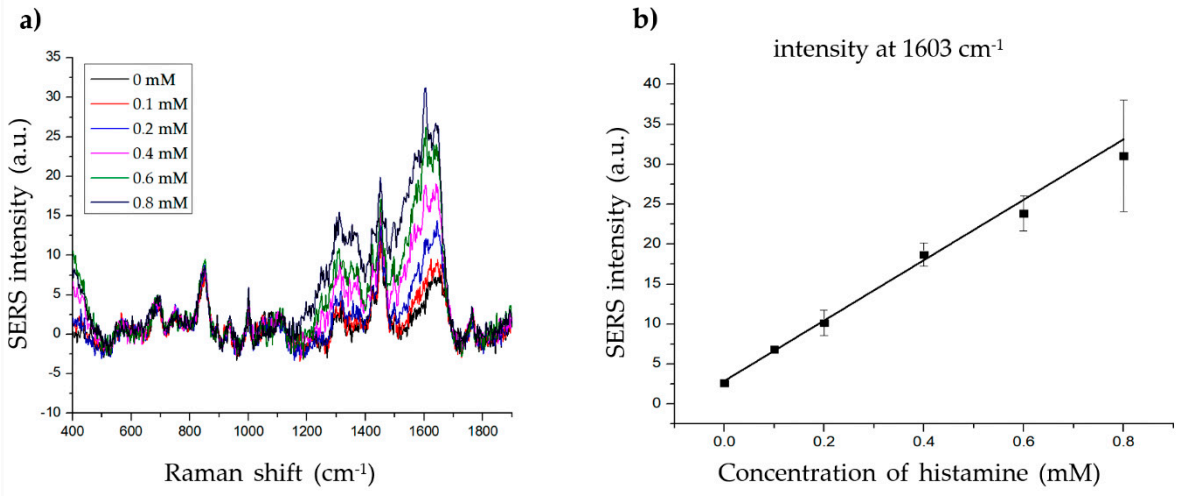

Figure 6. Determining the limit of detection (LOD) of histamine. (**a**) The Raman signal of histamine at different concentrations (0, 0.1, 0.2, 0.4, 0.6, and 0.8 mM). (**b**) The standard linear plot of histamine concentration vs. SERS intensity at 1603 cm^{-1}.

3. Materials and Methods

3.1. Chemicals and Materials

All reagents were used as received from the suppliers without further purification. Tetraethylorthosilicate (TEOS), 3-aminopropyltriethoxysilane (APTS), polyvinylpyrrolidone (PVP) (Mw 40,000), silver nitrate ($AgNO_3$), L-ascorbic acid, Tween 20, tetrakis(hydroxymethyl)phosphonium chloride (THPC), gold (III) chloride trihydrate ($HAuCl_4$), and histamine dihydrochloride were purchased from Sigma-Aldrich (St. Louis, MO, USA). Ethyl alcohol (EtOH) and aqueous ammonium hydroxide (NH_4OH) were purchased from Daejung (Siheung, South Korea). HCl and NaOH were purchased from Samchun (Pyeongtaek, South Korea). Phosphate-buffered saline (PBS; 20×) was purchased from Dyne Bio (Seongnam,

South Korea). Ultrapure water (resistivity 18.2 MΩ×cm) was produced using a Millipore water purification system (EXL water purification, Vivagen Co., Ltd., Seongnam, South Korea).

3.2. Preparation of SiO_2@Au@Ag NPs

The SiO_2@Au@Ag NP material was prepared using silica NPs produced via the Stöber method, with an average diameter of approximately 160 nm. Following amine-functionalization performed by incubating a mixture containing 200 mg of silica NPs, 4 mL of absolute EtOH, 200 µL of APTS, and 40 µL of NH_4OH for 12 h, the silica NPs were incubated with Au NPs (2–3 nm) prepared by reducing $HAuCl_4$ with THPC for 12 h with gentle shaking at 25 °C. The surfaces of the aminated silica NPs were covered with Au NPs. An Ag shell was created on the surface of the SiO_2@Au NPs by reducing $AgNO_3$ in the presence of ascorbic acid and PVP; 200 µL of 200 µg/mL SiO_2@Au@Ag NPs were well dispersed in 9.8 mL of 1 mg/mL PVP solvent and then 20 µL of 10 mM $AgNO_3$ was added, followed by the addition of 20 µL of 10 mM ascorbic acid. This suspension was slowly stirred for 15 min for the reduction of Ag^+ ions to Ag. The reaction was repeated to obtain an $AgNO_3$ concentration of 300 µM. The SiO_2@Au@Ag NPs were collected by centrifugation at 8500 rpm for 15 min. Following several washes with EtOH to remove excess reagent, the SiO_2@Au@Ag NPs were re-dispersed in absolute EtOH to obtain a 200 µg/mL SiO_2@Au@Ag NP solution.

3.3. Histamine Detection

The histamine solution was prepared by dissolving histamine dihydrochloride in PBS-Tween 20 (1%; PBS-T), pH 7. To absorb histamine on the surface of the SiO_2@Au@Ag NPs, 100 µL of a 1 mM histamine solution were incubated with 100 µL of a 200 µg/mL SiO_2@Au@Ag NP suspension for 2 h, followed by centrifugation for 15 min at 11,000 rpm to collect the colloids. The NPs was washed several times with PBS-T (pH 7) to remove excess reagent. The SiO_2@Au@Ag@Histamine NPs were re-dispersed in 100 µL of PBS-T (pH 7) to obtain a 200 µg/mL SiO_2@Au@Ag@Histamine NP suspension. For optimization, each condition, including incubation time, solvent pH, and volume of histamine solution, was changed. The LOD of histamine was determined by varying the concentration of histamine. The control sample (baseline) consisted of only SiO_2@Au@Ag NP material in PBS-T (pH 7) solvent. Each experiment was conducted three times.

3.4. SERS Measurement of SiO_2@Au@Ag@Histamine

The SERS signals were measured using a DXR 2 Raman Microscope System (Thermo Fisher Scientific, Waltham, MA, USA) with a 532-nm laser excitation source and 10× objective lens. Liquid samples were measured in a capillary tube with a laser power of excitation of 10 mW for 5 s. The size of the laser beam spot was approximately 2.0 µm and the sites were randomly selected. The SERS spectra were collected in the 400–1900 cm^{-1} wavenumber range. Each sample was measured three times. The highest peak at wave number 1603 cm^{-1} was selected for analysis.

4. Conclusions

In this study, histamine was successfully detected by SERS using a SiO_2@Au@Ag alloy nanomaterial. The best SERS signal was obtained using an incubation time of 2 h, a material-to-histamine solution volume ratio of 1:5, PBS-T solvent at pH 7, and material concentration of 0.125 mg/mL; using this protocol, the LOD of histamine was 3.698 ppm. To the best of our knowledge, this study is the first to report histamine detection using gold-silver alloy-embedded silica nanoparticles and provides the basis for further research that could be applied to the detection of histamine in real samples. In addition, this study demonstrates that nanoalloys are novel materials that could have a broad application in the future.

Supplementary Materials: Supplementary materials can be found at http://www.mdpi.com/1422-0067/21/11/4048/s1.

Author Contributions: Conceptualization and experimental design, X.-H.P., B.-H.J., W.-Y.R. and K.-H.H.; investigation, K.-H.H., A.J., B.S., and Y.-H.K.; reagents and materials, J.A. and H.-M.K.; data analysis, X.-H.P., B.-H.J., and K.-H.H.; writing, K.-H.H., E.H., J.K. and B.S.S.; supervision, B.-H.J. All authors have read and agreed to the published version of the manuscript.

Funding: This research was funded by Konkuk University, 2017.

Acknowledgments: We wish to thank the Microbial Carbohydrate Resource Bank (MCRB, Seoul, Korea) for their consulting services.

Conflicts of Interest: The authors declare no conflict of interest.

Abbreviations

$AgNO_3$	Silver nitrate
APTS	3-Aminopropyltriethoxysilane
CE	Capillary electrophoresis
ELISA	Enzyme linked immunosorbent assay
EtOH	Ethyl alcohol
EU	European Union
FDA	U.S. Food and Drug Administration
$HAuCl_4$	Gold (III) chloride trihydrate
HCl	Hydrochloric acid
HPLC	High-performance liquid chromatography
LOD	Limit of detection
NaOH	Sodium hydroxide
NH_4OH	Ammonium hydroxide
NPs	Nanoparticles
PBS-T	Phosphate-buffered saline-Tween 20
PVP	Polyvinylpyrrolidone
S/N	Signal to noise ratio
SERS	Surface-enhanced Raman scattering
SiO_2@Au@Ag	Gold–silver alloy-embedded silica
TEM	Transmission electron microscopy
TEOS	Tetraethylorthosilicate
THPC	Tetrakis(hydroxymethyl)phosphonium chloride

References

1. Janči, T.; Valinger, D.; Kljusurić, J.G.; Mikac, L.; Filipec, S.V.; Ivanda, M. Determination of histamine in fish by Surface Enhanced Raman Spectroscopy using silver colloid SERS substrates. *Food Chem.* **2017**, *224*, 48–54. [CrossRef] [PubMed]
2. Chu, B.Q.; Lin, L.; He, Y. Rapid determination of histamine concentration in fish (Miichthys Miiuy) by surface-enhanced Raman spectroscopy and density functional theory. *Int. J. Agric. Biol. Eng.* **2017**, *10*, 252–258.
3. Kolosovas-Machuca, E.S.; Cuadrado, A.; Ojeda-Galván, H.J.; Ortiz-Dosal, L.C.; Hernández-Arteaga, A.C.; Rodríguez-Aranda, M.D.C.; Navarro-Contreras, H.R.; Alda, J.; Gonzalez, F. Detection of histamine dihydrochloride at low concentrations using Raman spectroscopy enhanced by gold nanostars colloids. *Nanomaterials* **2019**, *9*, 211. [CrossRef] [PubMed]
4. Tan, A.; Zhao, Y.; Sivashanmugan, K.; Squire, K.; Wang, A.X. Quantitative TLC-SERS detection of histamine in seafood with support vector machine analysis. *Food Control.* **2019**, *103*, 111–118. [CrossRef] [PubMed]
5. Xie, Z.; Wang, Y.; Chen, Y.; Xu, X.; Jin, Z.; Ding, Y.; Yang, N.; Wu, F. Tuneable surface enhanced Raman spectroscopy hyphenated to chemically derivatized thin-layer chromatography plates for screening histamine in fish. *Food Chem.* **2017**, *230*, 547–552. [CrossRef] [PubMed]

6. Rahimi, E.; Nayebpour, F.; Alian, F. Determination of histamine in canned tuna fish using ELISA method. *Am. Eurasian J. Toxicol. Sci.* **2012**, *4*, 64–66.
7. Nadeem, M.; Naveed, T.; Rehman, F.; Xu, Z. Determination of histamine in fish without derivatization by indirect reverse phase-HPLC method. *Microchem. J.* **2019**, *144*, 209–214. [CrossRef]
8. Muscarella, M.; Magro, S.L.; Campaniello, M.; Armentano, A.; Stacchini, P. Survey of histamine levels in fresh fish and fish products collected in Puglia (Italy) by ELISA and HPLC with fluorimetric detection. *Food Control.* **2013**, *31*, 211–217. [CrossRef]
9. Cinquina, A.; Longo, F.; CalìA; De Santis, L.; Baccelliere, R.; Cozzani, R. Validation and comparison of analytical methods for the determination of histamine in tuna fish samples. *J. Chromatogr. A* **2004**, *1032*, 79–85. [CrossRef]
10. Jinadasa, B.K.K.K.; Jayasinghe, G.; Ahmad, S. Validation of high-performance liquid chromatography (HPLC) method for quantitative analysis of histamine in fish and fishery products. *Cogent Chem.* **2016**, *2*, 1156806. [CrossRef]
11. Manz, G.; Booltink, E. Validation study of a HistaSure (TM) ELISA(Fast Track) for the determination of histamine in fish samples. *J. AOAC Int.* **2014**, *97*, 1601–1614. [CrossRef] [PubMed]
12. Çulha, M.; Cullum, B.; Lavrik, N.; Klutse, C.K. Surface-enhanced Raman scattering as an emerging characterization and detection technique. *J. Nanotechnol.* **2012**, *2012*. [CrossRef]
13. Schlücker, S. Surface-enhanced Raman spectroscopy: Concepts and chemical applications. *Angew. Chem. Int. Ed.* **2014**, *53*, 4756–4795. [CrossRef] [PubMed]
14. Wang, Y.; Yan, B.; Chen, L. SERS tags: Novel optical nanoprobes for bioanalysis. *Chem. Rev.* **2012**, *113*, 1391–1428. [CrossRef]
15. Cai, X.-L.; Liu, C.; Liu, J.; Lu, Y.; Zhong, Y.-N.; Nie, K.; Xu, J.-L.; Gao, X.; Sun, X.-H.; Wang, S.-D. Synergistic effects in CNTs-PdAu/Pt trimetallic nanoparticles with high electrocatalytic activity and stability. *Nano Micro Lett.* **2017**, *9*, 48. [CrossRef]
16. Ferrando, R.; Jellinek, J.; Johnston, R.L. Nanoalloys: From theory to applications of alloy clusters and nanoparticles. *Chem. Rev.* **2008**, *108*, 845–910. [CrossRef] [PubMed]
17. Karthikeyan, B.; Loganathan, B. Rapid green synthetic protocol for novel trimetallic nanoparticles. *J. Nanoparticles* **2013**, *2013*. [CrossRef]
18. Khan, Z. Trimetallic nanoparticles: Synthesis, characterization and catalytic degradation of formic acid for hydrogen generation. *Int. J. Hydrogen Energy* **2019**, *44*, 11503–11513. [CrossRef]
19. Ye, X.; He, X.; Lei, Y.; Tang, J.; Yu, Y.; Shi, H.; Wang, K. One-pot synthesized Cu/Au/Pt trimetallic nanoparticles with enhanced catalytic and plasmonic properties as a universal platform for biosensing and cancer theranostics. *Chem. Commun.* **2019**, *55*, 2321–2324. [CrossRef]
20. Devi, P.; Patil, S.D.; Jeevanandam, P.; Navani, N.K.; Singla, M.L. Synthesis, characterization and bactericidal activity of silica/silver core–shell nanoparticles. *J. Mater. Sci. Mater. Electron.* **2014**, *25*, 1267–1273. [CrossRef]
21. Kandpal, D.; Kalele, S.; Kulkarni, S.K. Synthesis and characterization of silica-gold core-shell (SiO2@Au) nanoparticles. *Pramana* **2007**, *69*, 277–283. [CrossRef]
22. Nghiem, T.H.L.; Le, T.N.; Do, T.H.; Vu, T.T.D.; Do, Q.H.; Tran, H.N. Preparation and characterization of silica–gold core–shell nanoparticles. *J. Nanoparticle Res.* **2013**, *15*. [CrossRef]
23. Pol, V.G.; Gedanken, A.; Calderon-Moreno, J. Deposition of gold nanoparticles on silica spheres: A sonochemical approach. *Chem. Mater.* **2003**, *15*, 1111–1118. [CrossRef]
24. Purdy, S.C.; Muscat, A.J. Coating nonfunctionalized silica spheres with a high density of discrete silver nanoparticles. *J. Nanoparticle Res.* **2016**, *18*, 70. [CrossRef]
25. Roy, S.; Dixit, C.K.; Woolley, R.; O'Kennedy, R.; McDonagh, C. Synthesis and characterization of model silica–gold core–shell nanohybrid systems to demonstrate plasmonic enhancement of fluorescence. *Nanotechnology* **2012**, *23*, 325603. [CrossRef] [PubMed]
26. Tang, S.; Tang, Y.; Zhu, S.; Lu, H.; Meng, X. Synthesis and characterization of silica–silver core–shell composite particles with uniform thin silver layers. *J. Solid State Chem.* **2007**, *180*, 2871–2876. [CrossRef]
27. Zhu, M.; Qian, G.; Hong, Z.; Wang, Z.; Fan, X.; Wang, M. Preparation and characterization of silica–silver core-shell structural submicrometer spheres. *J. Phys. Chem. Solids* **2005**, *66*, 748–752. [CrossRef]

28. Zienkiewicz-Strzałka, M.; Deryło-Marczewska, A.; Kozakevych, R.B. Silica nanocomposites based on silver nanoparticles-functionalization and pH effect. *Appl. Nanosci.* **2018**, *8*, 1649–1668. [CrossRef]
29. Hahm, E.; Cha, M.G.; Kang, E.J.; Pham, X.-H.; Lee, S.H.; Kim, H.-M.; Kim, D.-E.; Lee, Y.-S.; Jeong, D.H.; Jun, B.-H. Multilayer Ag-embedded silica nanostructure as a surface-enhanced Raman scattering-based chemical sensor with dual-function internal standards. *ACS Appl. Mater. Interfaces* **2018**, *10*, 40748–40755. [CrossRef]
30. Hahm, E.; Jeong, D.; Cha, M.G.; Choi, J.M.; Pham, X.H.; Kim, H.M.; Kim, H.; Lee, Y.S.; Jeong, D.H.; Jung, S.; et al. beta-CD dimer-immobilized Ag assembly embedded silica nanoparticles for sensitive detection of polycyclic aromatic hydrocarbons. *Sci. Rep. UK* **2016**, *6*, 26082. [CrossRef]
31. Hahm, E.; Kang, E.J.; Pham, X.H.; Jeong, D.; Jeong, D.H.; Jung, S.; Jun, B.H. Mono-6-deoxy-6-aminopropylamino-beta-cyclodextrin on Ag-embedded SiO2 nanoparticle as a selectively capturing ligand to flavonoids. *Nanomater. Basel* **2019**, *9*, 1349. [CrossRef] [PubMed]
32. Jun, B.H.; Kim, G.; Jeong, S.; Noh, M.S.; Pham, X.H.; Kang, H.; Cho, M.H.; Kim, J.H.; Lee, Y.S.; Jeong, D.H. Silica core-based surface-enhanced Raman scattering (SERS) tag: Advances in multifunctional SERS nanoprobes for bioimaging and targeting of biomarkers. *B Korean Chem. Soc.* **2015**, *3*, 963–978.
33. Kang, E.J.; Baek, Y.M.; Hahm, E.; Lee, S.H.; Pham, X.H.; Noh, M.S.; Kim, D.E.; Jun, B.H. Functionalized beta-cyclodextrin immobilized on Ag-embedded silica nanoparticles as a drug carrier. *Int. J. Mol. Sci.* **2019**, *20*, 315. [CrossRef] [PubMed]
34. Kim, T.H.; Pham, X.-H.; Rho, W.-Y.; Kim, H.-M.; Hahm, E.; Ha, Y.; Son, B.S.; Lee, S.H.; Jun, B.-H. Ag and Ag-Au introduced silica-coated magnetic beads. *Bull. Korean Chem. Soc.* **2018**, *39*, 250–256. [CrossRef]
35. Pham, X.-H.; Hahm, E.; Kang, E.; Na Ha, Y.; Lee, S.H.; Rho, W.-Y.; Lee, Y.-S.; Jeong, D.H.; Jun, B.-H. Gold-silver bimetallic nanoparticles with a Raman labeling chemical assembled on silica nanoparticles as an internal-standard-containing nanoprobe. *J. Alloys Compd.* **2019**, *779*, 360–366. [CrossRef]
36. Pham, X.-H.; Hahm, E.; Kim, H.-M.; Shim, S.; Kim, T.H.; Jeong, D.H.; Lee, J.-Y.; Jun, B.-H. Silver nanoparticle-embedded thin silica-coated graphene oxide as an SERS substrate. *Nanomaterials* **2016**, *6*, 176. [CrossRef]
37. Pham, X.-H.; Hahm, E.; Kim, H.-M.; Son, B.; Jo, A.; An, J.; Thi, T.T.; Nguyen, D.; Jun, B.-H. Silica-coated magnetic iron oxide nanoparticles grafted onto graphene oxide for protein isolation. *Nanomaterials* **2020**, *10*, 117. [CrossRef]
38. Pham, X.-H.; Hahm, E.; Kim, T.H.; Kim, H.-M.; Lee, S.H.; Lee, Y.-S.; Jeong, D.H.; Jun, B.-H. Enzyme-catalyzed Ag growth on Au nanoparticle-assembled structure for highly sensitive colorimetric immunoassay. *Sci. Rep.* **2018**, *8*, 6290. [CrossRef]
39. Pham, X.-H.; Lee, M.; Shim, S.; Jeong, S.; Kim, H.-M.; Hahm, E.; Lee, S.H.; Lee, J.-Y.; Jeong, D.H.; Jun, B.-H. Highly sensitive and reliable SERS probes based on nanogap control of a Au–Ag alloy on silica nanoparticles. *RSC Adv.* **2017**, *7*, 7015–7021. [CrossRef]
40. Pham, X.-H.; Shim, S.; Kim, T.-H.; Hahm, E.; Rho, W.-Y.; Jeong, D.H.; Lee, J.-Y.; Jun, B.-H.; Kim, H.-M. Glucose detection using 4-mercaptophenyl boronic acid-incorporated silver nanoparticles-embedded silica-coated graphene oxide as a SERS substrate. *BioChip J.* **2016**, *11*, 46–56. [CrossRef]
41. Pham, X.-H.; Hahm, E.; Huynh, K.-H.; Kim, H.-M.; Son, B.S.; Jeong, D.H.; Jun, B.-H. Sensitive and selective detection of 4-aminophenol in the presence of acetaminophen using gold–silver core–shell nanoparticles embedded in silica nanostructures. *J. Ind. Eng. Chem.* **2020**, *83*, 208–213. [CrossRef]
42. Shim, S.; Pham, X.-H.; Cha, M.G.; Lee, J.-Y.; Jeong, D.H.; Jun, B.-H. Size effect of gold on Ag-coated Au nanoparticle-embedded silica nanospheres. *RSC Adv.* **2016**, *6*, 48644–48650. [CrossRef]
43. Bastús, N.G.; Merkoçi, F.; Piella, J.; Puntes, V. Synthesis of highly monodisperse citrate-stabilized silver nanoparticles of up to 200 nm: Kinetic control and catalytic properties. *Chem. Mater.* **2014**, *26*, 2836–2846. [CrossRef]
44. Pham, X.-H.; Hahm, E.; Huynh, K.-H.; Son, B.; Kim, H.-M.; Jeong, D.H.; Jun, B.-H. 4-Mercaptobenzoic acid labeled gold-silver-alloy-embedded silica nanoparticles as an internal standard containing nanostructures for sensitive quantitative thiram detection. *Int. J. Mol. Sci.* **2019**, *20*, 4841. [CrossRef]
45. Collado, J.A.; Ramírez, F.J. Vibrational spectra and assignments of histamine dication in the solid state and in solution. *J. Raman Spectrosc.* **2000**, *31*, 925–931. [CrossRef]

46. Davis, K.L.; McGlashen, M.L.; Morris, M.D. Surface-enhanced Raman scattering of histamine at silver electrodes. *Langmuir* **1992**, *8*, 1654–1658. [CrossRef]
47. Itabashi, M.; Shoji, K.; Itoh, K. Raman spectra of copper(II)-histamine (1:2) and nickel(II)-histamine (1:2) aqueous solutions. *Inorg. Chem.* **1982**, *21*, 3484–3489. [CrossRef]
48. Janči, T.; Mikac, L.; Ivanda, M.; Radovčić, N.M.; Medić, H.; Filipec, S.V. Optimization of parameters for histamine detection in fish muscle extracts by surface-enhanced Raman spectroscopy using silver colloid SERS substrates. *J. Raman Spectrosc.* **2016**, *48*, 64–72. [CrossRef]
49. Ramírez, F.J.; Tuñón, I.; Collado, J.A.; Silla, E. Structural and vibrational study of the tautomerism of histamine free-base in solution. *J. Am. Chem. Soc.* **2003**, *125*, 2328–2340. [CrossRef]
50. Torreggiani, A.; Tamba, M.; Bonora, S.; Fini, G. Raman and IR study on copper binding of histamine. *Biopolymers* **2003**, *72*, 290–298. [CrossRef]
51. Peycheva, M.; Yankovska, T.; Stoilova, N. HPLC/FL method for histamine testing in fish. In Proceedings of the Book Days of Veterinary Medicine 2012 3rd International Scientific Meeting, Ohrid, North Macedonia, 2–4 September 2012.